ASSESSMENT OF THE EFFECTS OF TUBE CURRENT AND VOLTAGE INTENSITY, OF THE POSITION AND METAL TYPE ON THE OCCURRENCE OF METAL ARTEFACTS IN CBCT SECTION

Andreea Băluță[1], Anca-Oana Dragomirescu[1*], Maria-Angelica Bencze[1], Adriana Vasilache[1], Marina Imre[2], Ecaterina Ionescu[1]

[1]Department of Orthodontics and Dentofacial Orthopedics, Faculty of Dental Medicine, "Carol Davila" University of Medicine and Pharmacy, 020021 Bucharest, Romania;
[2] Department of Complete Denture, Faculty of Dental Medicine, "Carol Davila" University of Medicine and Pharmacy, 020021 Bucharest, Romania; marina.imre@umfcd.ro;

*Correspondence: anca.dragomirescu@umfcd.ro (A.O.D.)

Introduction

Cone Beam Computed Tomography (CBCT) has been recommended for dental imaging in preoperative implant evaluation as it provides a high-quality three-dimensional image without magnification or distortion with a relatively low radiation dose, making it extremely useful for assessing bone and making accurate measurements. [1,2] Due to artifact production, postoperative implant evaluation using CBCT technology is often compromised.[3,4]

Image artefacts are inconsistent in the imaging data that do not correspond to the physical characteristics of the object being assessed. Their occurrence is related to the technical aspects of the CBCT scanner, but also to the composition of the scanned object which generates a significant effect, as it can act as a filter that modifies the X-ray spectrum, depending on the number and atomic density of the constituent material. [5] Artefacts are problematic, especially in the dentoalveolar area, due to the frequent presence of metallic objects such as metallic restorative materials, coronal root restorations, crowns, brackets, and dental implants. These artefacts are produced due to the high density of the metal, which is above the normal limit a computer can measure. Because metals strongly attenuate X-ray beams, beam attenuation in structures adjacent to metal structures is not recorded correctly. Due to image reconstruction techniques in 3D modalities such as computed tomography (CT) and CBCT, the presence of metal in scanned areas causes various image damage, ranging from bright streaks radiating from metal objects, to blackening of adjacent areas or complete loss of grey value between adjacent metal objects. As a result, the region of interest for diagnosis, treatment plan, monitoring is not visually adequate. [6]

The cone beam in CBCT leads to artifacts in all directions around metal objects [6,7]. Since a goal in the use of CBCT is the accurate measurement and observation of anatomical structural details, evaluation of methods that can reduce metal artifacts is of particular

importance. There have been studies in this context, however, most of these studies have focused on the use of artifact reduction algorithms [8-11]. Although these types of software programs would remove streaks away from the metal object, the details around the metal-tissue interface, which may be the primary region of interest (ROI), may not yet be visible to clinicians [12]. Among the effective factors considered in image quality, exposure parameters are adjustable in some CBCT units. Despite this, only a few studies have focused on the effect of exposure parameters on metal artifacts [7,13,14,15], also the effects of different metal structures positioned at the jaw [7,16] and metal type [13,17] have been evaluated less frequently. The aim of this study was to evaluate the effects of tube current intensity and kilovoltage (kVp) of the CBCT unit, position of metal objects in the jaw and metal type on metal artefacts in cone-beam computed tomography (CBCT) images.

Material and Method

In this study, the impact of exposure parameters (milliamperage and kilovoltage) of the CBCT unit, the type of metal and the position of metal structures inserted at the jaw were evaluated. The study was performed on an acrylic model, using 3 metal rods each of cobalt-chromium-titanium alloy, 2.8 mm in diameter and 15 mm high. The Ti rods were used for the evaluation of artefacts induced by dental implants, the Cr-Co rods for the evaluation of artefacts arising from coronal root restorations. Titanium rods were made of Titanium Ti6Al4V (manufacturer NTI-Kahla GmbH, Germany). For maximum accuracy and dimensional similarity, the fabrication of the chromium-cobalt alloy rods was carried out using CAD-CAM technology. Parallel holes with dimensions corresponding to the fabricated rods were milled in the mandible in the canine area, the area of the second premolar and the distal root of the 6-year molar at equal distances from each other. To simulate radiation attenuation in soft tissues, the bone area was coated with wax approximately 15 mm thick. Prior to the CBCT purchases, the model was fixed on the machine platform, on the basis provided by the manufacturer. The model was placed in the FOV centre and aligned with the horizontal plane using the laser light system for orientation. Scout images were taken before scanning to ensure correct model placement (Fig. 1). In the first step, the scanning of the control model without inserted metal rods was performed using different currents in intensity (1mA, 5mA, 10mA) and different voltages (60kV, 70kV, 80kV) with field of view (FOV) 4 x 4 and 0.16 voxel size of the Morita Veraviewepocs 3De unit (J. Morita, Kyoto, Japan), then the titanium rods were placed. Subsequently the process was repeated with cobalt-chromium alloy rods. The exposure parameters used are shown in Table I.

Figure 1

Table I

TITAN ΔGV										
			pozitia							
protocol	FOV	voxel	molar L	molar V	pm L	pm V	canin L	canin V	c-pm	pm-m
60kV,1mA	4x4	0.16	4.8	-9.55	-11.15	-6.92	-32.24	-5.38	-46.12	-36.01
60kV,5mA	4X4	0.16	2.96	-9.31	-8.78	-7.59	-25.84	-6.06	-37.76	-29.84
60kV,10mA	4X4	0.16	-13.92	-35.76	-27.04	-32.55	-47.17	-30.5	-66.36	-56.58
70kV,1mA	4X4	0.16	-11.25	-21.3	-19.01	-18.97	-30.44	-16.94	-44.48	-37.88
70kV,5mA	4X4	0.16	-10.76	-24.89	-16.23	-21.91	-38.29	-19.99	-54.04	-44.18
70kV,10mA	4X4	0.16	-10.52	-25.22	-21.2	-17.55	-40.52	-16.91	-46.2	-39.53
80kV,1mA	4X4	0.16	6.19	-10.6	-5.2	-7.62	-23.94	-6.28	-31.21	-23.55
80kV,5mA	4X4	0.16	7.53	-8.47	-0.72	-4.39	-20.24	-0.01	-32.65	-23.44
80kV,10mA	4X4	0.16	14.67	7.79	-3.76	8.05	-11.66	7.88	-23.74	-17.17
ALIAJ ΔGV										
			pozitia							
protocol	FOV	voxel	molar L	molar V	pm L	pm V	canin L	canin V	c-pm	pm-m
60kV,1mA	4X4	0.16	-14.05	-21.02	-32.47	-23.41	-37.85	-20.25	-65.17	-63.43
60kV,5mA	4X4	0.16	17.77	1.58	-1.03	-0.22	-6.5	7.67	-43.65	-41.86
60kV,10mA	4X4	0.16	28.07	11.29	16.05	15.44	16.26	16.2	-24.52	-21.25
70kV,1mA	4X4	0.16	1.71	-11.31	-15.5	-7.84	-9.54	-1.75	-40.07	-38.33
70kV,5mA	4X4	0.16	22.14	-7.19	0.45	0.62	-3.43	12.53	-44.81	-42.58
70kV,10mA	4X4	0.16	19.71	16.23	3.54	12.83	8.59	20.65	-35.23	-32.71
80kV,1mA	4X4	0.16	20.09	6.89	2.15	7.17	-4.18	16.69	-22.41	-21.32
80kV,5mA	4X4	0.16	9.74	5.21	-6.92	4.06	-17.69	10.06	-36.68	-35.1
80kV,10mA	4X4	0.16	44.26	36.57	15.38	39.23	17.87	47.97	-15.78	-13.05

All reconstructions were selected at the same axial level. The axial plane perpendicular to the rod located in the premolar area, located at 3 mm from the surface, was selected as the reference plane. The default axial images were exported as uncompressed multi-frame images in Digital Imaging and Communications in Medicine (DICOM) format from proprietary software (iDixel image processing software, J. Morita USA, Inc, Irvine, USA) and imported into Image J software for analysis and saved as a "png" image in a two-dimensional form used for comparison (Fig. 2).

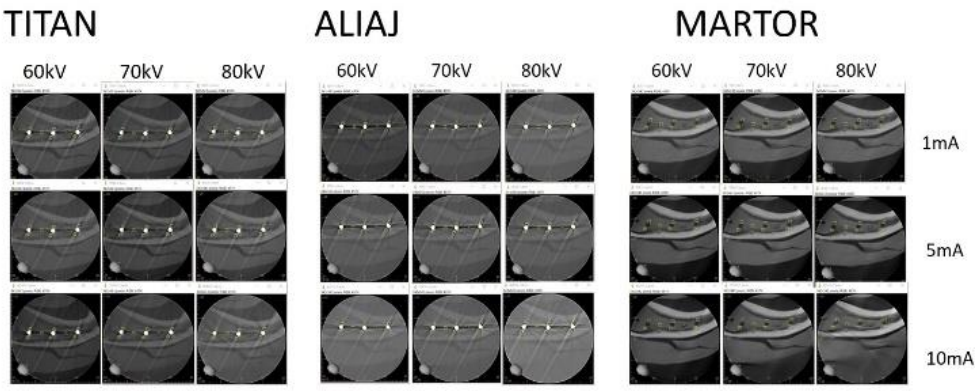

Figure2

CBCT image assessment

The two-dimensional images were numbered, in no specific order, and given for analysis to two observers who selected eight 10 x 10-pixel rectangular areas considered as ROIs (regions of interest). These regions include the regions adjacent to the vestibular apex of the rods, the lingual surface and the midline regions corresponding to an imaginary line connecting the anterior and middle rods, respectively the middle and posterior rods. (fig.3)

Figure 3

Images were evaluated using Image J software (NIH Image) and grey values were measured in the eight regions of each image. Observers evaluated each image twice. To assess inter-observer and intra-observer agreement, a correlation

coefficient (absolute correlation type) was performed, and it was 99.9%.

On each axial image, the histogram was calculated using a macro function, so that regions of interest (ROI) were standardized for all images. The mean grey level (GV) and standard deviation of the ROIs were determined, and image quality was measured as the percentage difference between the grey values (ΔGV%) on the control and test models.

The Benic et al. method [4] was used to study the effect of beam hardening around implants by comparing the mean circumferential grey values around implants. This methodology was adapted for use in this research. The average GV measured in the ROI defined on the control model for each scan parameter was designated as GVcontrol. Differences in grey values (ΔGV) between models with metal rods (GVTest) and without (GVcontrol) were calculated as percentages using the following formula:

ΔGV% = [(GVTest - GVcontrol)/GVcontrol] * 100

Statistical analysis

To evaluate the effects of the four factors (voltage, current, type of metal, position of objects) in the occurrence of metal artefacts, interactions (double, triple, quadruple in most cases) were calculated. An independent t-test was used to compare the material effect (dichotomous variable). Prior to analysis, pooled independent variables were analysed for normality (Kolmogorov-Smirnov test) and equal variances (F-test for normally distributed data and Levene's test for abnormally distributed data). To detect the relevance of the difference between GVtest and GVcontrol, the 95% confidence interval (CI) for ΔGV values was calculated. If the value "0" was not contained in the 95% CI, there was statistical evidence that the mean ΔGV value was different from "0" at a 0.05 significance level. For comparison of other factors with more than two categories, one-way ANOVA tests were used, then Tukey's or Gawes-Hawell's test for pairwise comparison. The significant level was considered to be < 0.05. Data for ΔGV alloy and titanium and are presented in Table I.

Results

Two approaches were used to analyse the data:

- To visualize and describe the trends for each metal type, descriptive statistics which materialized in the representation of two graphs (fig.4, fig.5),

- Statistical comparison for the effects of the classified independent variables.

The working hypothesis was represented by ΔGV% as an index of image quality. Interpretation of values for ΔGV% was as follows:

- ΔGV% close to zero (0) means that there is little or no difference in image quality between the model without inserts (control) and the model with inserts (test),

- -ΔGV% describes a relative hyper-dense or dark region associated with beam hardening and,

- + ΔGV% is a relative hypo-dense or bright region associated with scattered radiation.

Image quality for titanium

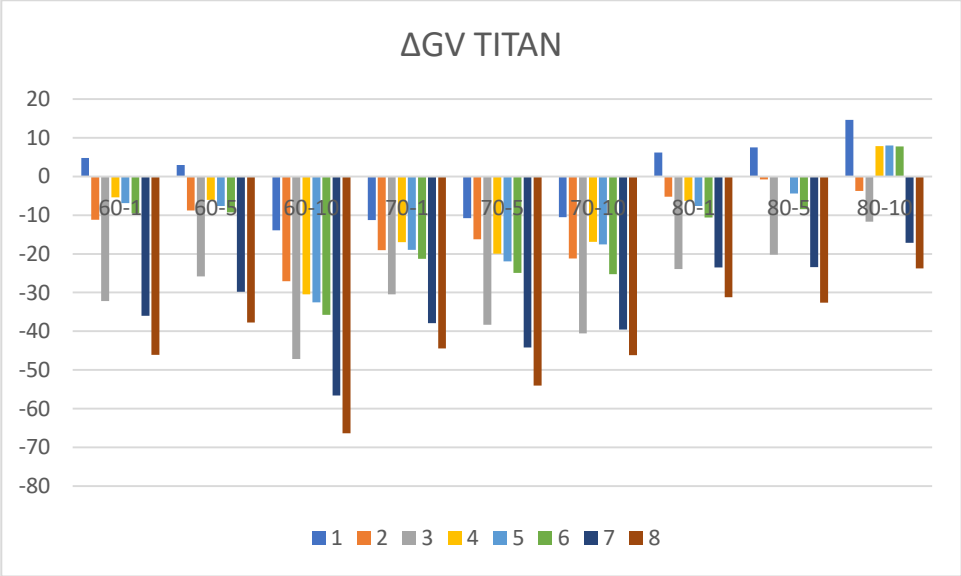

Figure 4: *Total ΔGV% graph for titanium.*

For image quality (ΔGV%), in general, for titanium, the following are noted:

- quality is generally reduced due to metal effects by increasing the overall image density due to beam hardening (-ΔGV%),

- beam hardening effects are predominant (in 64 out of 72 positions),

- the effects occur independently of rod position,

- effects are generated independently of kV and mA,

- the greatest deterioration in image quality occurs in the positions of the midline regions corresponding to the image line connecting the anterior and middle and middle and posterior rods, followed by the lingual area of the canine,

- the increase in kV resulted in reduced artefacts in the positions adjacent to the lingual and buccal rods ($P < 0.00014$),

- in all titanium samples, artefacts between the middle and anterior rods were more intense than in the region between the posterior and middle rods ($P<0.05$)

Image quality for cobalt-chromium alloy

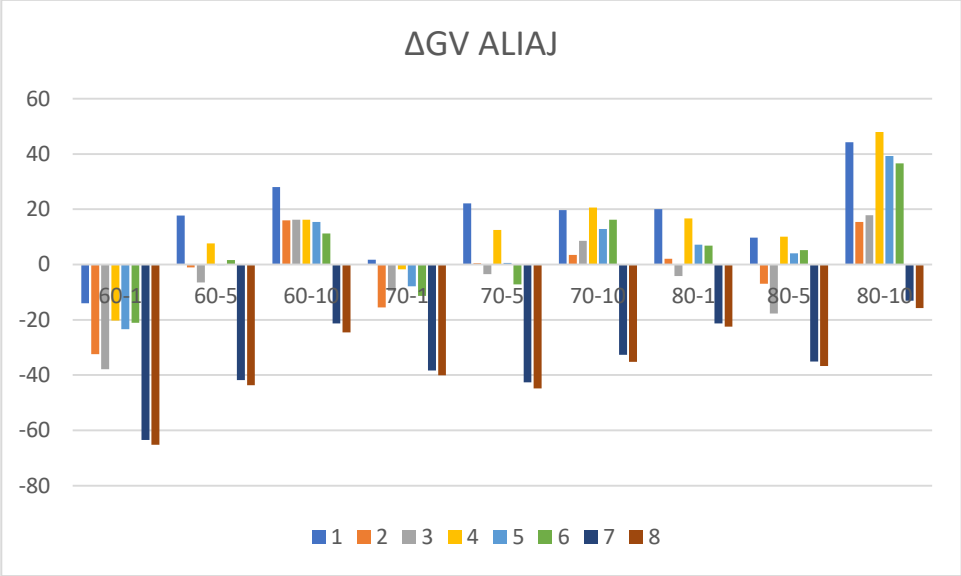

Figure 5 Total ΔGV% graph for cobalt chrome alloy

Image quality (ΔGV%) for cobalt chromium alloy:

- Artifact presence is independent of rod position,

- cobalt-chromium alloy produced significantly more intense artefacts than titanium at all positions ($p < 0.000040$),

- beam hardening effects are lower compared to titanium (-ΔGV%) and scattering effects become higher,

- the scattering effects are visible in most of the buccal and oral rod positions (in 36 out of 54 positions).

- There were no significant differences in the comparison of the 'posterior to middle rod' position with the 'middle to anterior rod' position in all conditions ($P > 0.05$).

- Values adjacent to the posterior lingual and anterior buccal rod were significantly higher than the other two intermediate positions ($P < 0.00003$).

- the change in tension did not result in a reduction in artefacts ($P>0.05$),

ANOVA and post-hoc tests indicated that alloy rods produced more artefacts than titanium rods, according to standard deviation values ($p < 0.00004$), (Fig. 6). The change in tube current intensity did not affect artefacts ($P>0.05$), except for the lingual area of the anterior rod ($P=0.03$). Increasing kVp generally resulted in a reduction of metal artefacts ($P = 0.04$) in positions adjacent to the anterior and posterior rods in particular (Fig. 7), with no significant impact in intermediate positions between the posterior and middle rods and between the middle and anterior rods.

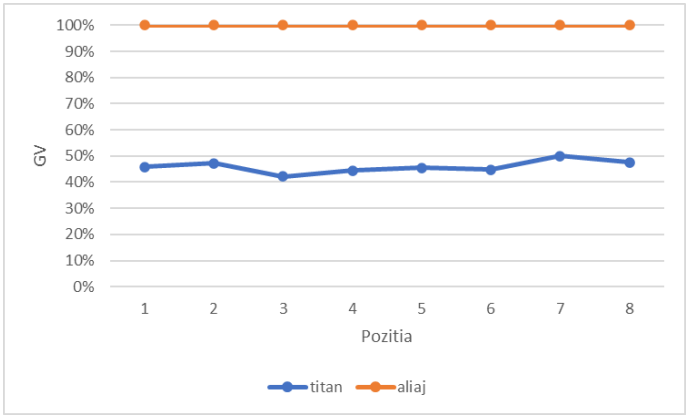

Figure 6 Mean and standard deviations of grey values in CBCT images due to metal artifacts induced by different types of metal at different positions of metal objects, regardless of kVp and mA.

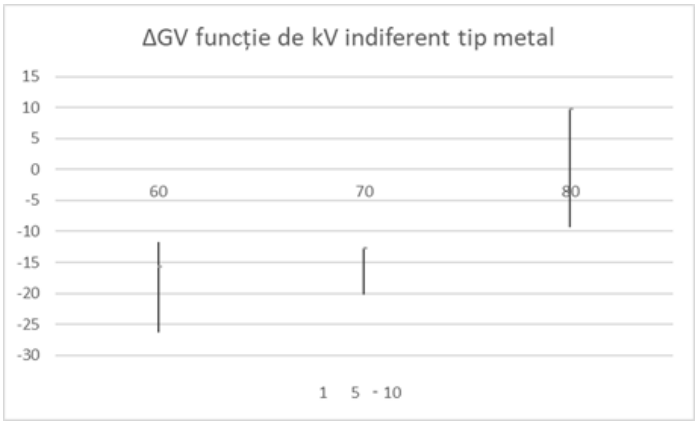

Figure 7 ΔGV depending on kV regardless of the type of metal inserted

Discussions

In general, when a beam of polychromatic X-rays passes through an object, low energy photons are absorbed more than high energy photons. This phenomenon increases the average energy of the X-ray beam, causes the beam to harden and disturbs the image reconstruction process. A lower X-ray beam energy, a higher density, and an irradiated substance with a higher atomic number lead to more beam hardening, and thus more severe artefacts when metal is present. [5,18]. This is because when X-ray beams pass simultaneously through two metal rods, beam hardening will be more severe [20,22]. According to the results of this study between the two metal rods anterior and middle and middle and posterior respectively, quenching artefacts and lower grey values are observed. In this study, the metal artifacts adjacent to the anterior buccal and posterior lingual rods were more intense than those of the other positions, which could be due to different projection paths, information processing and reconstruction techniques. It is possible that there are different results when using different CBCT units, as seen in studies by Schulze et al, [3] and Benic et al, [4] where implant site did not affect artifact severity.

This in vitro study was designed to provide a quantitative analysis of the effects of CBCT image artefacts produced by high density objects using a simulated model of the mandibular dental arch scanned at different CBCT system acquisition parameters. Titanium and cobalt-chromium alloy rods were positioned in three representative tooth locations (canine, second premolar and distal root of the first molar) at the mandibular arch using nine (9) exposure parameter configurations.

The grey values measured at eight (8) specific locations, were compared with the grey values of the control model (without any metal insert) to arrive at ΔGV%, which could be statistically compared with each other. ΔGV% was thus used as an index of image quality. The ΔGV% value of "0" meant that the inserted metal rods had no significant effect on image quality. Values + ΔGV% meant that the images were brighter than the control images in the areas evaluated and were thus affected by scattering. The - ΔGV% values indicated that the images were affected by beam hardening and were darker than the control images. Using these values as a reference, conclusions were drawn as to whether an independent variable affected image quality.

Comparisons between titanium and cobalt-chromium revealed that at all eight positions and using all exposure parameters, artifacts induced by the cobalt-chromium rods were more intense than those observed in the titanium exposures. Cobalt-chromium-induced missing value artifacts were more severe than those of titanium in the region between the middle and anterior rods, but both this position and that between the posterior and middle rods generated the most intense artifacts in both conditions. Thus, the grey value between the two cobalt-chromium or titanium inserts with different exposure parameters underwent the largest changes. The photoelectron absorption occurred refers to the atomic number cube of the irradiated substance. Since the atomic numbers of chromium (24) and cobalt (27) are higher than that of titanium (22) and there are metals with a higher atomic number used in cobalt-chromium alloys (e.g., molybdenum and tungsten), the X-ray absorption and beam hardening were higher than for titanium. Studies by Pauwels et al, [13] Kuusisto et al. [22] reported that lead and stainless steel, zirconium, and titanium, respectively, produced severe artefacts on CBCT images. The study by Chindasombatjareon et al, [17] evaluated the artefacts produced by four metals and it was observed that gold alloy type IV caused the largest areas of artefacts followed by cobalt alloy, chromium, titanium, and aluminium.

According to the results of this study increasing kVp generally resulted in a reduction of metal artefacts in positions adjacent to the anterior and posterior rods but did not affect artefact severity in positions between rods. Previous studies [7,12, 17,21] have found that increasing the voltage generates higher energy and greater penetration of the X-ray beam, so there is less beam hardening and fewer metal artifacts. High kVp also reduces contrast, which can contribute to greater image homogeneity. Other factors that could affect beam hardening include the rotational arc of the machine, the X-ray

beam configuration, and the algorithms used for information processing [19,23].

Similar to Pauwels' study [13] the increase in current intensity did not affect the presence of metal artefacts in most cases, with the exception of the lingual area of the anterior rod, where an inversion of ΔGV occurred. In Kataoka's study [21], using CT, higher tube currents decreased metal artefacts, however, we have to consider the intensity range used in that study (100-500mA), which was different from that used in the present study (1-10mA). Since CBCT shows a narrow range of mA changes it can explain the insignificant effect of mA change on metal artefacts.

Conclusions

Metal type had the greatest effect on the intensity of metal artefacts in this study, with cobalt-chromium alloy-induced artefacts being more severe than titanium-induced artefacts, and those scans were more affected by the different protocols than titanium. Artifacts were more intense on the buccal surface of the anterior rods for titanium and on the lingual surface of the posterior rod for alloy. Increasing the tube current had no effect on metal artefacts. This highlights how the protocols act differently for each metal object inserted at the oral cavity, and how the choice of acquisition protocol can influence image quality, especially for high atomic number metal inserts, taking into account the type of material present in the scan region, the image quality needed for diagnosis and the radiation dose to the patient.

References

1. Kamburoğlu K, Kiliç C, Ozen T, Yüksel SP. Measurements of man- dibular canal region obtained by cone-beam computed tomogra- phy: A cadaveric study. Oral Surg Oral Med Oral Pathol OralRadiolEndod2009;107:e34–e42.
2. Angelopoulos C, Aghaloo T. Imaging technology in implant diag- nosis. Dent Clin North Am 2011;55:141–158.
3. Schulze RK, Berndt D, d'Hoet B. On cone-beam computed tomog- raphy artifacts induced by titanium implants. Clin Oral Implants Res 2010;21:100–107.
4. Benic GI, Sancho-Puchades M, Jung RE, Deyhle H, Hämmerle CH. In vitro assessment of artifacts induced by titanium dental implants in cone beam computed tomography. Clin Oral Implants Res 2013;24:378–383.
5. Schulze R, Heil U, Gross D, et al. Artefacts in CBCT: A review. Dento- maxillofac Radiol 2011;40:265–273.
6. Jaju PP, Jain M, Singh A, Gupta A. Artefacts in cone beam CT. Open J Stomatol. 2013 Jul;3(05):292.
7. Schulze RK, Berndt D, d'Hoedt B. On cone-beam computed tomography artifacts induced by titanium implants. Clin Oral Implants Res. 2010 Jan;21(1): 100-7.
8. Bechara B, McMahan CA, Geha H, Noujeim M. Evaluation of a cone beam CT artefact reduction algorithm. Dentomaxillofac Radiol. 2012 Jul;41(5): 422-8.
9. Gong XY, Meyer E, Yu XJ, Sun JH, Sheng LP, Huang KH, et al. Clinical evaluation of the normalized metal artefact reduction algorithm caused by dental fillings in CT. Dentomaxillofac Radiol. 2013;42(4):20120105.
10. Ibraheem I. Reduction of artifacts in dental cone beam CT images to improve the three dimensional image reconstruction. J Biomed Sci Eng. 2012 Aug;5 (8):409-15.

11. Bechara BB, Moore WS, McMahan CA, Noujeim M. Metal artefact reduction with cone beam CT: an in vitro study. Dentomaxillofac Radiol. 2012 Mar;41 (3):248-53.
12. Barrett JF, Keat N. Artifacts in CT: recognition and avoidance. Radiographics. 2004 Nov-Dec;24(6): 1679-91.
13. Pauwels R, Stamatakis H, Bosmans H, Bogaerts R, Jacobs R, Horner K, et al. Quantification of metal artifacts on cone beam computed tomography images. Clin Oral Implants Res. 2013 Aug;24 Suppl A100:94-9.
14. Katsumata A, Hirukawa A, Noujeim M, Okumura S, Naitoh M, Fujishita M, et al. Image artifact in dental cone-beam CT. Oral Surg Oral Med Oral Pathol Oral Radiol Endod. 2006 May;101(5):652-7.
15. Panjnoush M, Kheirandish Y, Kashani PM, Fakhar HB, Younesi F, Mallahi M. Effect of Exposure Parameters on Metal Artifacts in Cone Beam Computed Tomography. J Dent (Tehran). 2016 Jun;13(3):143-150. PMID: 28392810; PMCID: PMC5376540.
16. Benic GI, Sancho-Puchades M, Jung RE, Deyhle H, Hammerle CH. In vitro assessment of artifacts induced by titanium dental implants in cone beam computed tomography. Clin Oral Implants Res. 2013 Apr;24(4):378-83.
17. Chindasombatjareon J, Kakimoto N, Murakami S, Maeda Y, Furukawa S. Quantitative analysis of metallic artifacts caused by dental metals: comparison of cone-beam and multi-detector row CT scanners. Oral Radiol. 2011 Dec;27(2):114-20.
18. Pauwels R, Araki K, Siewerdsen JH, Thongvigitmanee SS. Technical aspects of dental CBCT: state of the art. Dentomaxillofac Radiol. 2015;44(1):20140224.
19. Hunter A, McDavid D. Analyzing the beam hardening artifact in the Planmeca Promax. Oral Surg Oral Med Oral Pathol Oral Radiol Endod. 2009 Apr;107(4):e28-9.
20. White SC, Pharoah MJ. Oral radiology: principles and interpretation. 7th Ed., St. Louis, Missouri, Elsevier-Mosby, 2014:196.
21. Kataoka ML, Hochman MG, Rodriguez EK, Lin PJ, Kubo S, Raptopolous VD. A review of factors that affect artifact from metallic hardware on multi-row detector computed tomography. Curr Probl Diagn Radiol. 2010 Jul-Aug;39(4):125-36.
22. Kuusisto N, Vallittu PK, Lassila LV, Huumonen S. Evaluation of intensity of artefacts in CBCT by radio-opacity of composite simulation models of implants in vitro. Dentomaxillofac Radiol. 2015;44(2):20140157
23. Schulze D, Heiland M, Blake F, Rother U, Schmelzle R. Evaluation of quality of reformatted images from two cone-beam computed tomographic systems. J Craniomaxillofac Surg. 2005 Feb;33(1): 19-2